# RESPONSES TO EDITOR:

Thank you very much for all your technical corrections and comments. Next, we add the marked manuscript with all your corrections:

# Statistical Analysis for Satellite Index-Based Insurance to define Damaged Pasture Thresholds

**Juan José Martín-Sotoca[1]*, Antonio Saa-Requejo[2,3], Rubén Moratiel[2,3], Nicolas Dalezios[4], Ioannis Faraslis[5], and Ana María Tarquis[2,6]**

jmartinsotoca@gmail.com, antonio.saa@upm.es, ruben.moratiel@upm.es, dalezios.n.r@gmail.com, faraslisgiannis@yahoo.gr, anamaria.tarquis@upm.es

[1] Data Science Laboratory. European University, Madrid, Spain.
[2] CEIGRAM, Research Centre for the Management of Agricultural and Environmental Risks, Madrid, Spain.
[3] Dpto. Producción Agraria. Universidad Politécnica de Madrid, Spain.
[4] Department of Civil Engineering. University of Thessaly, Volos, Greece.
[5] Department of Planning and Regional Development. University of Thessaly, Volos, Greece.
[6] Grupo de Sistemas Complejos. Universidad Politécnica de Madrid, Spain.

* Correspondence to: jmartinsotoca@gmail.com

**Abstract:** Vegetation indices based on satellite images, such as Normalized Difference Vegetation Index (NDVI), have been used in countries like USA, Canada and Spain for damaged pasture and forage insurance for the last years. This type of agricultural insurance is called "satellite index-based insurance" (SIBI). In SIBI, the occurrence of damage is defined through NDVI thresholds mainly based on statistics derived from Normal distributions. In this work a pasture area at the north of Community of Madrid (Spain) has been delimited by means of Moderate Resolution Imaging Spectroradiometer (MODIS) images. A statistical analysis of NDVI histograms was applied to seek for alternative distributions using maximum likelihood method and $\chi^2$ test. The results show that the Normal distribution is not the optimal representation and the General Extreme Value (GEV) distribution presents a better fit through the year based on a quality estimator. A comparison between Normal and GEV are showed respect to the probability under a NDVI threshold value along the year. This suggests that a priori distribution should not be selected and a percentile methodology should be used to define a NDVI damage threshold rather than the average and standard deviation, typically of Normal distributions.

**Keywords:** NDVI, pasture insurance, GEV distribution, MODIS.

## Highlights

- The GEV distribution provides better fit to the NDVI historical observations than the Normal one.
- Difference between Normal and GEV distributions are higher during spring and autumn, transition periods in the precipitation regimen.
- NDVI damage threshold shows evident differences using Normal and GEV distributions covering both the same probability (24.20%).

- NDVI damage threshold values based on percentiles calculation is proposed as an improvement in the index based insurance in damaged pasture.

## 1. Introduction

Agricultural insurance addresses the reduction of the risk associated with crop production and animal husbandry. The concept of index-based insurance (IBI) attempts to achieve settlements based on the value taken by an objective index rather than on a case-by-case assessment of crop or livestock losses (Gommes and Kayitakier, 2013). Indeed, the goal of IBI policy remains to develop an affordable tool to all producers, including smallholders. Specifically, IBI can constitute a safety net against weather-related risks for all members of the farming community, thereby increasing food security and reducing the vulnerability of rural populations to weather extremes. Moreover, IBI can be associated with credits for insured smallholders, due to the fact that the risk of non-repayment for lenders is reduced, which encourages the use of agricultural inputs and equipment, leading to increased and more stable crop production. Over the past decade, the importance of weather index-based insurances (WIBI) for agriculture has been increasing, mainly in developing countries (Gommes and Kayitakier, 2013). This interest can be explained by the potential that IBI constitutes a risk management instrument for small farmers. Indeed, it can be considered within the context of renewed attention to agricultural development as one of the milestones of poverty reduction and increased food security, as well as the accompanying efforts from various stakeholders to develop agricultural risk management instruments, including agricultural insurance products.

Farmers need to protect their land and crops specifically from drought in arid and semi-arid countries, since their production may directly depend mainly on the impacts of this particular natural hazard. Insurance for drought-damaged lands and crops is currently the main instrument and tool that farmers can resort in order to deal with agricultural production losses due to drought. Many of these insurances are using satellite vegetation indices (Rao, 2010), thus they are also called “satellite index-based insurances” (SIBI). SIBI have some advantages over WIBI, such as cost-effective information and acceptable spatial and temporal resolution. They do not, however, resolve the issue of basis risk, i.e. potential unfairness to insurance takers (Leblois, 2012). Moreover, the very nature of an index-based product creates the chance that an insured party may not be paid when they suffer loss. For this reason, in some countries (Spain) they have named this SIBI as “damaged in pasture” to cover not only drought even this one is the main cause.

It is highly recognized that shortage of water has many implications to agriculture, society, economy and ecosystems. Specifically, its impact on water supply, crop production and rearing of livestock is substantial in agriculture. Knowing the likelihood of drought is essential for impact prevention (Dalezios, 2013). Drought severity assessment can be approached in different ways: through conventional indices based on meteorological data, such as temperature, rainfall, moisture, etc. (Niemeyer, 2008), as well as through remote sensing indices based on images usually taken by artificial satellites (Lovejoy et al., 2008) or drones. In the second group they are found Satellite Vegetation Indices (SVI), which can quantify "green vegetation", and soil moisture through Soil Water Index (Gouveia et al., 2009) combining different spectral reflectances. Thus, they are one of the main ways to quantitatively assess drought severity.

At the present time, several satellites (NOAA, TERRA, DEIMOS, etc.) can provide this spectral information with different spatial resolution. Some series with a high temporal frequency are freely available, those from NOAA satellites and Terra. The most widely known SVI is the Normalized Difference Vegetation Index (NDVI). It follows the principle that healthy vegetation mainly reflects the near-infrared frequency band. There are several other important SVI, such as Soil Adjusted Vegetation Index (SAVI) and Enhanced Vegetation Index (EVI) that incorporate soil effects and atmospheric impacts, respectively. An important point of SIBI is "when damage occurs". To measure this, a SVI threshold value is defined mainly based on statistics that apply to Normal distributed variables: average and standard deviation. When current SVI values are bellow this threshold value for a period of time, insurance recognizes that a damage is occurring, most of the times drought, and then it begins to pay compensations to farmers.

Important NDVI-based indices for detecting drought are NDVI anomalies (NDVIA) and Standardized Vegetation Index (SVI). NDVIA and SVI have been successfully used to monitor drought conditions over different regions in the world (Nanzad et al., 2019; Li et al., 2014). NDVIA is calculated as the difference between the NDVI value for a specific time period (e.g., week, month) and the long-term mean value for that period. SVI was developed by Peters et al. (2002) and obtains the probability from normal NDVI distributions over multiple years of data, on a time period (Anyamba and Tucker, 2012; Bayarjargal et al., 2006). It is defined as:

$$SVI_i = \frac{NDVI_i - \overline{NDVI}}{\sigma_{NDVI}} = \frac{NDVIA_i}{\sigma_{NDVI}} \quad (1)$$

where $\overline{NDVI}$ is the long-term mean NDVI in the period i, $\sigma_{NDVI}$ is the standard deviation of NDVI in the period i, and $NDVI_i$ is the current NDVI value in the time period i. Using

only the first and second statistical moment, average and the square root of variance, the assumption of normality is implicit in this type of drought NDVI indicator. The normality assumption is challenged in this study.

WIBI aims to protect farmers against weather-based disasters such as droughts, frosts and floods. A WIBI policy links possible insurance payouts with the weather requirements of the crop being insured: the insurer pays an indemnity whenever the realized value of the weather index meets a specified threshold. Whereas payouts in traditional insurance programs are related to actual crop damages, a farmer insured under a WIBI contract may receive a payout. A current difficulty to the wide implementation of WIBI is the weakness of indices. Indeed, there is certainly a need for more efficient indices based on the additional experience gained from the implementation of WIBI products in the developing world. Current trends in index technology are exciting and they actuate high expectations, especially the development of yield indices and the use of remote sensing inputs. Risk protection and insurance illiteracy constitute another difficulty, which has to be addressed by training and awareness-raising at all levels, from farmers to farmers' associations, micro-insurance partners, as well as senior decision-makers in insurance, banking, and politics (Bailey, 2013). It is essential that all stakeholders (especially the insured) perfectly understand the principles of IBI, as otherwise the insurer, even the whole concept of insurance, is at risk of reputation loss for years or decades.

There is currently a lack of technical capacity in the insurance sectors of most developing countries, which is a constraint to the scaling up and further development of WIBI (Gommes and Kayitakire, 2012). Specifically, although it is possible to design an index product and assist in roll-out, marketing, and sales, such assistance is not possible on a wide scale, simply because there is lack of qualified expertise. Indeed, it usually requires mathematical modeling, data manipulation, and expertise in crop simulation to design an index. Nevertheless, it is possible to structure insurance with multiple indices, but this increases the complexity of the product and makes it difficult for farmers to comprehend it. 'Basis risk' is also a particular problem for index products, which is frequently caused by the fact that measurements of a particular variable, such as rain, may differ at the insurer's measurement site and in the farmer's field. This also creates problems for insurance providers. Indeed, part of the reason the scaling up of index products has failed is that both insurers and farmers suffer from this basis risk.

Currently, to mitigate impacts of climate-related reduced productivity of French grasslands, several studies have been developed to design new insurance scheme bases indemnity payouts to farmers on a forage production index (FPI) (Rumiguié et al., 2015;

2017). Two examples of SIBIs are presented in two different countries: USA and Spain. In particular, in USA there are several insurance programs for pasture, rangeland and forage, which use various indexing systems (rainfall and vegetation indices), and are promoted by Unites States Department of Agriculture (USDA) (Maples et al., 2016; USDA, 2018). NDVI is the index chosen in the vegetation index program and it is obtained from AVHRR (Advanced Very High Resolution Radiometer) sensor onboard NOAA satellites. Average, maximum and minimum NDVI values are obtained from a historical series with the aim of calculating a trigger value. Insurer decides the quantity of compensation comparing this trigger with current value. On the other hand, in Spain there exists the "Insurance for Damaged Pasture" from "Spanish System of Agricultural Insurance" (BOE, 2013). This insurance defines damage event through NDVI values obtained from MODIS sensor onboard TERRA satellite of NASA. In this insurance, NDVI threshold values ($NDVI_{th}$) are calculated subtracting several times ($k = 0.7\ or\ k = 1.5$) standard deviation to average within a homogeneous area:

$$NDVI_{th} = \mu - k \cdot \sigma \tag{2}$$

where $\mu, \sigma$ are average and standard deviation of NDVI respectively. Average and standard deviation come of supposing Normal distributions in the historical data (Goward et al., 1985; Hobbs, 1995; Fuller, 1998; Al-Bakri and Taylor, 2003; Turvey et al., 2012; De Leeuw et al. 2014).

The aim of this paper is to find a more realistic statistical NDVI distribution without the "a priori" assumption that variables follow a Normal distribution, typically for current SIBI methodology. In order to achieve this, the Maximum Likelihood Method (MLM) is fitted to a historical series of NDVI values in a pasture land area in Spain (Community of Madrid). Different types of asymmetrical distributions are examined with the aim to find a better fit than Normal. To eliminate some noise in the historical series, an original method is applied consisting of using Hue-Saturation-Lightness (HSL) color model. Finally, Chi-square test ($\chi^2$ test) has been used to check the goodness of fit for all considered distributions.

## 2. Materials and Methods

### 2.1 Vegetation Index

The differences of the reflectance of green vegetation in parts of the electromagnetic radiation spectrum, namely, visible and near infrared, provide an innovative method for monitoring surface vegetation from space. Specifically, the spectral behavior of vegetation cover in the visible (0.4-0.7mm) and near infrared (0.74-1.1mm, 1.3-2.5mm) offers the possibility to monitor from space the changes in the different stages of cultivated and uncultivated plants taking also into account the corresponding behavior of the surrounding microenvironment (Ortega-Farias et al., 2016). Indeed, from the visible part of the electromagnetic radiation spectrum it is possible to draw conclusions about the rate photosynthesis, whereas from near infrared inferences are extracted about the chlorophyll density and the amount of canopy in the plant mass, as well as the water content in the leaves, which is also linked directly to the rate of transpiration with impacts to physiological process of photosynthesis. Usually, data from NOAA/AVHRR series of polar orbit meteorological satellites are used with low spatial resolution (1.1 $km^2$) and recurrence interval at least twice daily from the same location. Several algorithms combining channels of red (RED), near infrared (NIR) and green (GREEN) have been proposed, which provide indices sensitive to green vegetation.

NDVI uses two frequency bands: red band (660 nm) and near-infrared band (860 nm). Absorption of red band is related to photosynthetic activity and reflectance of near-infrared band is related to presence of vegetation canopies (Flynn, 2006). In drought periods, NDVI values can reduce significantly, therefore many researchers have used this index to measure drought events in recent years (Dalezios et al., 2014). To calculate NDVI we will use this mathematical formula:

$$\boldsymbol{NDVI} = \frac{\boldsymbol{IR-R}}{\boldsymbol{IR+R}} \tag{3}$$

where “IR” and “R” are reflectance values in Near-Infrared band and Red band, respectively. NDVI values below zero indicate no photosynthetic activity and are characteristic of areas with large accumulation of water, such as rivers, lakes, or reservoirs. The higher is the NDVI value, the greater is the photosynthetic activity and vegetation canopies.

In this paper, the NDVI is used, which is widely known index with a multitude of applications over time. The NDVI is suited for monitoring of total vegetation, since it partly compensates the changes in light conditions, land slope and field of view (Kundu et al., 2016). In addition, clouds, water and snow show higher reflectance in the visible than in the near infrared, thus, they have negative NDVI values. Indeed, bare and rocky terrain

show vegetation index values close to zero. Moreover, the NDVI constitutes a measure of the degree of absorption by chlorophyll in the red band of the electromagnetic spectrum. In summary, the NDVI is a reliable index of the chlorophyll density on the leaves, as well as the percentage of the leaf area density over land, thus, NDVI constitutes a credible measure for the assessment of dry matter (biomass) in various species vegetation cover (Dalezios, 2013). It is clear from the above that the NDVI is an index closely related to growth and development of plants, which can effectively monitor surface vegetation from space.

The continuous increase of the NDVI value during the growing season reflects the vegetative and reproductive growth due to intense photosynthetic activity, as well as the satisfactory correlation with the final biomass production at the end of a growing period. On the other hand, gradual decrease of the NDVI values signifies stress due to lack of water or extremely high temperatures for the plants, leading to a reduction of the photosynthetic rate and ultimately a qualitative and quantitative degradation of plants. NDVI values above zero indicate the existence of green vegetation (chlorophyll), or bare soil (values around zero), whereas values below zero indicate the existence of water, snow, ice and clouds.

**2.2 Database**

Scientific research satellite Terra (EOS AM-1) has been chosen to provide necessary information to calculate NDVI in the study area. This satellite was launched into orbit by NASA on December 18, 1999. MODIS sensor aboard this satellite collects information of different reflectance bands. MODIS information is organized by "products". The product used in this study was MOD09A1 (LP DAAC, 2014). MOD09A1 incorporates seven frequency bands: Band 1 (620-670 nm), band 2 (841-876 nm), band 3 (459-479 nm), band 4 (545-565 nm), 5 band (1230-1250 nm), band 6 (1628-1652 nm) and band 7 (2105-2155 nm). The bands used to calculate NDVI are: band 1 for red frequency and band 2 for near-infrared frequency. MOD09A1 provides georeferenced images with pixel resolution of 500m x 500m. Each MOD09A1 pixel contains the best possible L2G observation during an 8-day period as selected on the basis of high observation coverage, low view angle, the absence of clouds or cloud shadow, and aerosol loading.

The period of time selected on this study was from 2002 to 2017.

Daily data from a principal station of the meteorological network were utilized during the period studied (2002 – 2017). Meteorological station is located in 40°41'46"N 3°45'54"W (elevation 1004 m a.s.l.), less than 2 km from the study area (AEMET, 2017).

## 2.3 Site description

Six pixels (500m x 500m) are considered located in a pasture area at the north of the Community of Madrid (Spain) between the municipalities of "Soto del Real" and "Colmenar Viejo". The study area is located between meridians 3° 45' 00" and 3° 47' 00" W and parallels 40° 42' 00" and 40° 44' 00" N approximately (see Fig. 1).

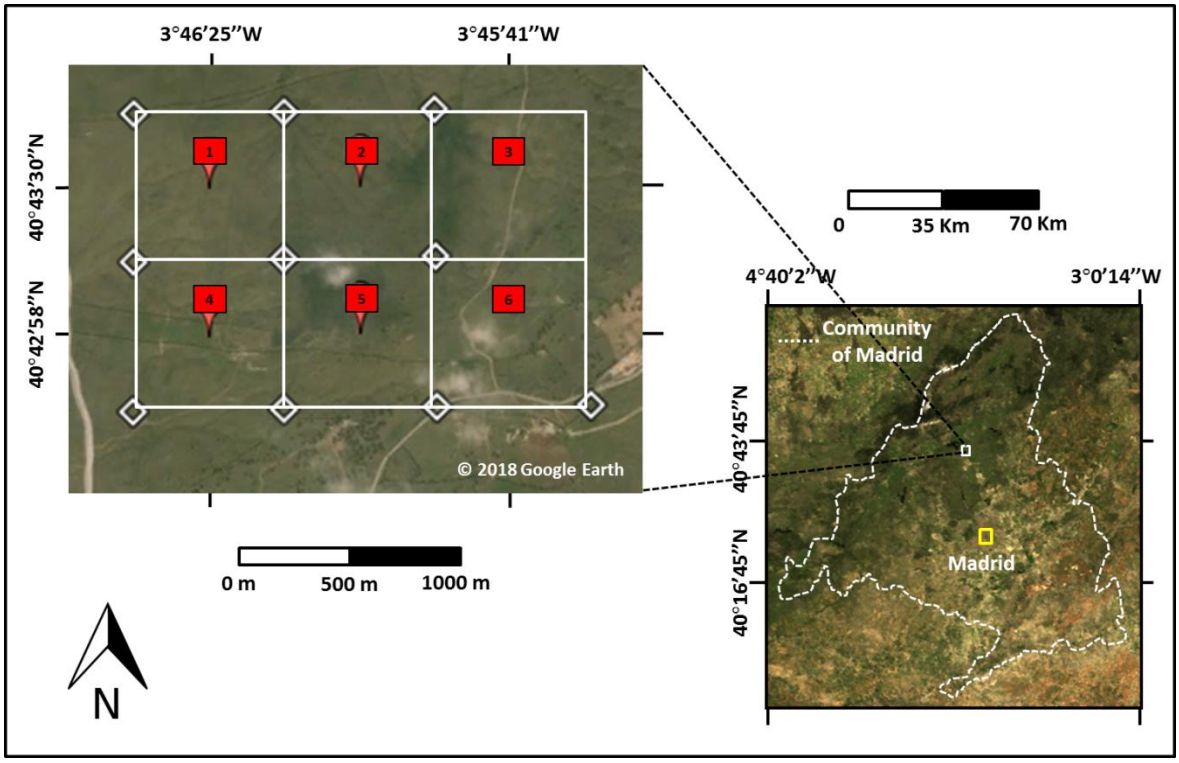


**Figure 1.** The study area is in the centre of the Iberian Peninsula (Community of Madrid). RGB image of six pixels area used for case study is shown (Google Earth´s and MODIS images).

The annual mean temperature ranges during the study period from 12.7°C to 13.8°C, and annual mean precipitation ranges from 360 mm to 781 mm. The stations studied were identified semi-arid (annual ratio P/ETo between 0.2 and 0.5) according to the global aridity index developed by the United-Nations Convention to Combat Desertification (UNEP, 1997). According to the climatic classification of Köppen (Kottek et al., 2006), this area presents a continental Mediterranean climate temperate with dry and temperate

summer (type Csb). Temperature and precipitation of this site, based on 20 years, is presented in Table 1.

Due to high soil moisture conditions, ash is the dominant tree, forming large agroforestry systems ("dehesas") that are used for pasture. These are ecosystems with high biodiversity.

**Table 1.** Monthly average of maximum temperature (Tmax), average temperature (Tavg), minimum temperature (Tmin) and precipitation (P). Study period from 1997 to 2017.

| Month | Jan | Feb | Mar | Apr | May | Jun | Jul | Aug | Sep | Oct | Nov | Dec | Annual |
|---|---|---|---|---|---|---|---|---|---|---|---|---|---|
| Tmax (ºC) | 7.1 | 9.3 | 12.7 | 15.4 | 19.5 | 24.6 | 28.6 | 28.1 | 23.7 | 16.8 | 11.1 | 7.4 | 17.0 |
| Tavg (ºC) | 3.6 | 4.8 | 7.7 | 10.1 | 13.7 | 18.4 | 22.0 | 21.7 | 17.9 | 12.3 | 7.1 | 4.1 | 12.0 |
| Tmin (ºC) | 0.0 | 0.3 | 2.6 | 4.8 | 7.8 | 12.1 | 15.4 | 15.3 | 12.0 | 7.8 | 3.0 | 0.8 | 6.8 |
| P (mm) | 67.2 | 50.0 | 38.5 | 62.2 | 62.3 | 30.2 | 18.9 | 16.4 | 34.2 | 79.3 | 86.2 | 82.6 | 627.9 |

## 2.4 HSL model

There is no doubt that NDVI time-series from satellite sensors carry useful information, which can be used for characterizing seasonal dynamics of vegetation (Fensholt et al., 2012; Forkel et al., 2013). However, due to unfavorable atmospheric conditions during the data acquisition, NDVI time-series curve often contains noise (Motohka et al., 2011; Park, 2013). Although most of the NDVI data products are temporally composited through maximum value compositing (MVC) method (Holben, 1986) to retain relatively cloud-free data, residual noise still exists in the data, which will affect the accuracy of the NDVI value.

Therefore, usually it is necessary to reconstruct of NDVI time-series before extracting information from the noisy data. There are several techniques that have been applied to reduce noise and reconstruct NDVI series, a summary of these can be found in Wei et al. (2016). In this study we applied a simple filtering method based on the Hue-Saturation-Lightness (HSL) color model inspired by the work presented by Tackenberd (2007).

HSL color model is a cylindrical representation of RGB (Red-Green-Blue) points. Their components are Hue (color type), Saturation (level of color purity) and Lightness (color luminosity). Hue is the angular component and it is more intuitive for humans since it is directly related to the color wheel (see Fig. 2).

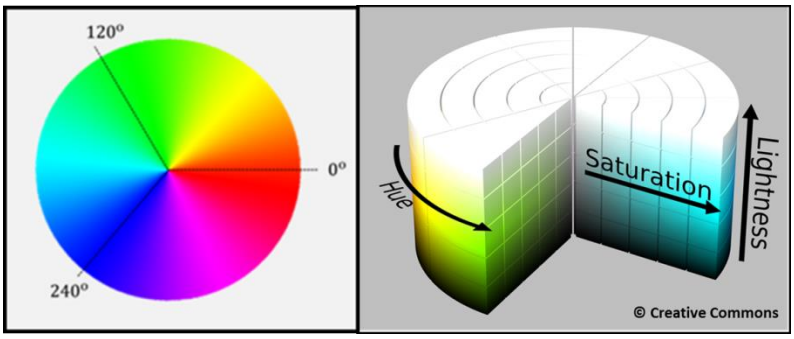


**Figure 2.** On the left: colour wheel of Hue. On the right: the HSL model (Creative Commons).

Saturation is the radial component and near-zero values indicate grey colors. Lightness is the axial radial versus axial component, zero lightness produces black and full lightness produces white.

The NDVI series are filtered using the following HSL criterion: NDVI values are valid if HSL Saturation is greater than 0.15. In this way, the values of the series that have grey color correlate with pasture covered by clouds or snow are eliminated. This type of filter based in HSL color space has been used on digital camera images monitoring vegetation phenology (Tackenberg, 2007; Crimmins and Crimmins, 2008; Graham et al., 2009). However, we have not found the use of this HSL criterion in the context of NDVI remote sensing images.

## 2.5 Maximum Likelihood Method

MLM estimates the set of parameters $\{\alpha, \beta, \mu, \sigma, \dots\}$ for a specific statistical distribution that maximizes the "likelihood function" or the "joint density function":

$$L = f(\boldsymbol{x}, \boldsymbol{\theta}) = \prod_{i=1}^{n} f(x_i; \alpha, \beta, \mu, \sigma, \dots) \quad (4)$$

where $\boldsymbol{x} = (x_1, \dots, x_n)$ is the set of data, $\boldsymbol{\theta} = (\alpha, \beta, \mu, \sigma, \dots)$ is the vector of parameters and $f(x_i; \alpha, \beta, \mu, \sigma, \dots)$ is the density function of the statistical model.

When maximization with respect to the vector of parameters is carried out, the estimated parameters $(\hat{\alpha}, \hat{\beta}, \hat{\mu}, \hat{\sigma}, \dots)$ for the proposed statistical distribution are obtained (Larson, 1982)**.** Properties of estimated parameters are: invariance, consistency and asymptotically unbiased.

In the case of a Normal model, the estimated statistics $\mu$ and $\sigma$ are defined by accurate expressions as follows:

$$\hat{\mu} = \bar{x} = \frac{1}{n}\sum_{i=1}^{n} x_i \qquad \hat{\sigma} = s = \sqrt{\frac{1}{n}\sum_{i=1}^{n}(x_i - \bar{x})^2} \tag{5}$$

where $\hat{\mu}$ is the sample mean and $\hat{\sigma}$ is the sample standard deviation of the data set.

In this study we will apply MLM to estimate the parameters for 4 probability density functions (PDF). In Table 2, a brief description is presented of these PDF candidates: Normal, Gamma, Beta and GEV. To do so, the following MATLAB functions have been used: "normfit", "gamfit", "betafit" and "gevfit" (respectively).

**Table 2.** Candidate Probability Density Functions (PDF).

| PDF NAME | PDF EXPRESSION | PDF PARAMETERS |
|---|---|---|
| Normal | $\mathbf{f(x;\mu,\sigma) = \frac{1}{\sigma\sqrt{2\pi}} e^{-\frac{1}{2}\left(\frac{x-\mu}{\sigma}\right)^2}}$ | $\boldsymbol{\mu \equiv average}$<br>$\boldsymbol{\sigma \equiv standard\ deviation}$ |
| Gamma | $\mathbf{f(x;\alpha,\beta) = \frac{1}{\beta^{\alpha}\Gamma(\alpha)} x^{\alpha-1} e^{-\frac{x}{\beta}}}$ | $\boldsymbol{\Gamma(.) \equiv gamma\ function}$<br>$\boldsymbol{\alpha}$ *and* $\boldsymbol{\beta \equiv parameters}$ |
| Beta | $\mathbf{f(x;a,b) = \frac{\Gamma(a+b)}{\Gamma(a)\Gamma(a)} x^{a-1}(1-x)^{b-1}}$ | $\boldsymbol{\Gamma(.) \equiv gamma\ function}$<br>$\boldsymbol{a}$ *and* $\boldsymbol{b \equiv parameters}$ |
| GEV | $\mathbf{f(x;\mu,\sigma,\xi) = \frac{1}{\sigma} t(x)^{\xi+1} e^{-t(x)}}$<br>where $\mathbf{t(x) = \begin{cases} \left(1 + \left(\frac{x-\mu}{\sigma}\right)\xi\right)^{-1/\xi} & \text{if } \xi \neq 0 \\ e^{-(x-\mu)/\sigma} & \text{if } \xi = 0 \end{cases}}$ | $\boldsymbol{\mu \in \mathbb{R} \equiv location\ param.}$<br>$\boldsymbol{\sigma > 0 \equiv scale\ parameter}$<br>$\boldsymbol{\xi \in \mathbb{R} \equiv shape\ parameter}$ |

## 2.6 Goodness of fit (Chi square test)

$\chi^2$ test can be used to determine to what extent observed frequencies differ from frequencies expected for a specific statistical model. The most important points of the theory are briefly presented in (Cochran, 1952).

Let $f(x,\theta)$ be a theoretical density function of a random variable X which depends on parameters $\theta = (\alpha, \beta, \mu, \sigma, \dots)$ and let $x_1, \dots, x_n$ be a sample of X grouped into k classes with $n_i$ data per class i.

Firstly, the following hypothesis is set:

($H_0$) observed data fit theoretical distribution $f(x,\theta)$.

Then the test statistic $\chi_c^2$ is defined as:

$$\chi_c^2 = \sum_{i=0}^{k} \frac{(n_i - e_i)^2}{e_i} \quad (6)$$

where $n_i$ is the number of data or observed frequency and $e_i = n \cdot P(class\ i)$ is the expected frequency for class i. $P(class\ i)$ is the theoretical interval probability defined for class i.

A level of significance is also set as:

$$\alpha = P(RejectH_0 \,/\, H_0 is\ true\ ) \quad (7)$$

Finally, the following decision rule is applied: "reject the theoretical distribution at significance level $\alpha$ if:

$$\chi_c^2 > \chi^2_{(k-m-1,1-\alpha)} \quad (8)$$

where $\chi^2_{(k-m-1,1-\alpha)}$ is a $\chi^2$ distribution with k-m-1 degrees of freedom (m is the number of parameters, k is the number of classes).

# 3. Results

## *3.1* HSL filtering criterion

NDVI series (from 2002 to 2017) were obtained for each pixel of the study area using frequency bands provided by MODIS product named MOD09A1. These series contain some irregular values that can skew NDVI pattern. Therefore, the six series (six pixels) were filtered using the HSL criterion.

MOD09A1 is a MODIS product that processes data to obtain the best observation in an 8-days period. However, it is possible that the result of this selection still presents some problems since the best of this selection is relative to the eight observations of the period. For example, if the eight observations, at one pixel, appear with clouds, shadow clouds or snow, the best selection still shows this problem.

As an example of the above, the NDVI series (10 years) of one pixel of the study area is shown in Fig. 3. On the top graph of Fig. 3 there are extremely low NDVI values in some dates. If these NDVI values are compared to neighbouring values (8 days after or before) the high variation presented in such short period is not plausible. This issue tells us that

394 the MODIS sensor has not obtained a proper observation during this 8 days period
395 (interval).
396
397 The HSL criterion helps us to eliminate these incorrect NDVI values, since the filter is
398 interpreting that these pixels still contains clouds or snow, i.e., pixels with low saturation
399 (greyish colours).
400
401

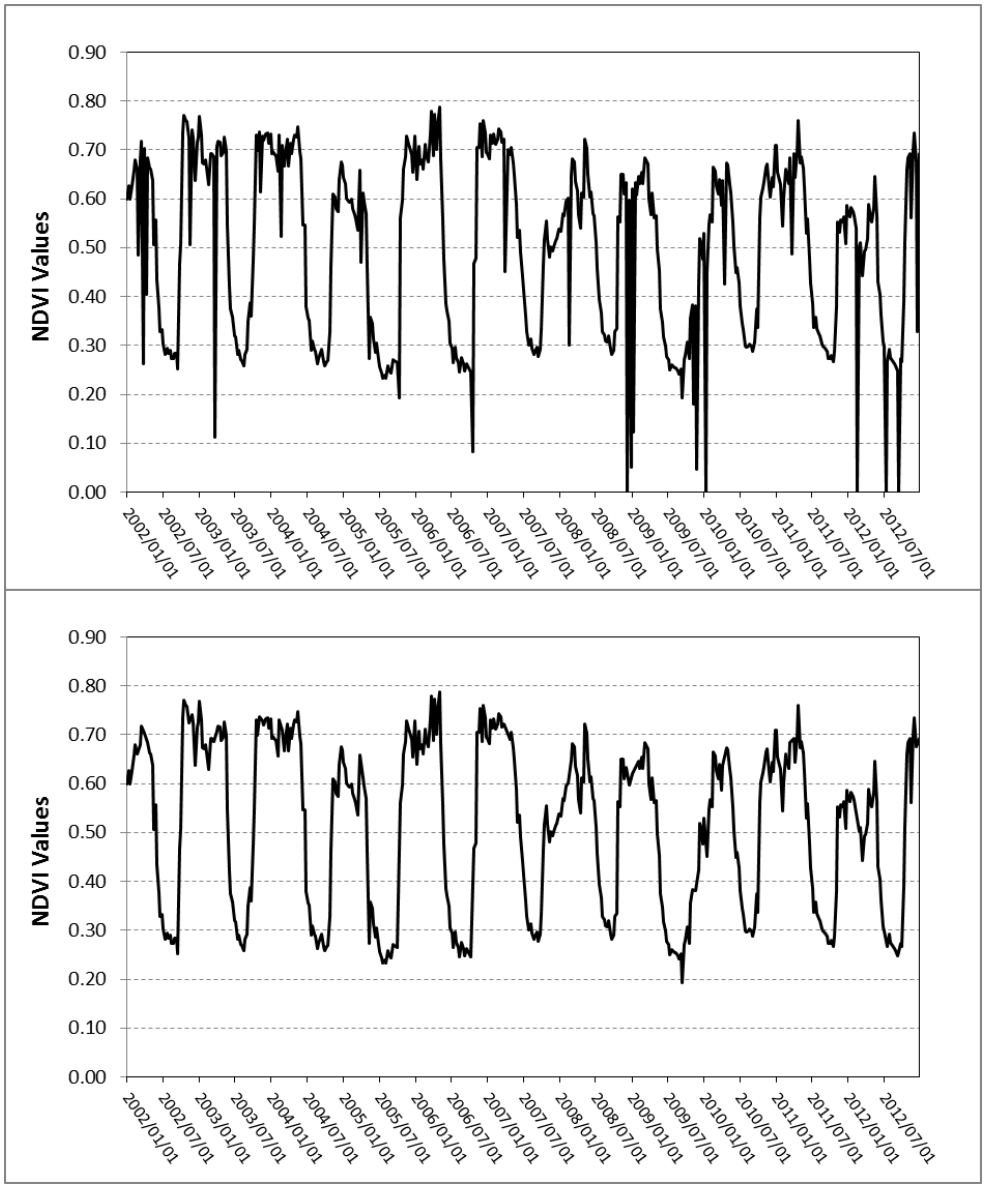


402
403 **Figure 3.** HSL filtering criterion applied to a 10 years NDVI series. Top graph shows the real NDVI
404 series. Bottom graph shows the HSL filtered NDVI series.

Fig. 3 shows that abrupt changes in the NDVI values, mainly observed during raining seasons such as autumn and winter, are efficiently eliminated. Not to be a high computational demanding method is one of the main advantages of HSL filtering method. Therefore, this method will allow us to obtain more robust NDVI values to be used in the statistical analysis.

### *3.2* Statistical analysis

NDVI values were obtained consecutively every 8 days from MODIS starting at the 1st of January of every year, in such a way that 46 NDVI observations were extracted for each year. Therefore, it was possible to define 46 Random Variables (RV) when all the years of this study were taking into account.

In Table 3, every RV (named as "Interval") is shown together with the number of available NDVI observations. Each RV collects the observations coming from the six selected pixels; therefore the maximum number of observations per RV could be: 6 pixels x 16 years = 96 observations. The start intervals of each season are: interval 45 (19 December) for winter, interval 11 (22 March) for spring, interval 23 (26 June) for summer and interval 34 (22 September) for autumn.

**Table 3.** Number of observations for every RV (named as Interval).

| RANDOM VARIABLE | # OBSERVATIONS | RANDOM VARIABLE | # OBSERVATIONS |
|---|---|---|---|
| **Interval 1** | 85 | **Interval 24** | 96 |
| **Interval 2** | 84 | **Interval 25** | 96 |
| **Interval 3** | 96 | **Interval 26** | 96 |
| **Interval 4** | 96 | **Interval 27** | 96 |
| **Interval 5** | 95 | **Interval 28** | 96 |
| **Interval 6** | 90 | **Interval 29** | 96 |
| **Interval 7** | 86 | **Interval 30** | 96 |
| **Interval 8** | 83 | **Interval 31** | 96 |
| **Interval 9** | 96 | **Interval 32** | 96 |
| **Interval 10** | 96 | **Interval 33** | 94 |
| **Interval 11** | 74 | **Interval 34** | 96 |
| **Interval 12** | 88 | **Interval 35** | 96 |
| **Interval 13** | 88 | **Interval 36** | 85 |
| **Interval 14** | 88 | **Interval 37** | 90 |
| **Interval 15** | 96 | **Interval 38** | 96 |
| **Interval 16** | 92 | **Interval 39** | 92 |
| **Interval 17** | 88 | **Interval 40** | 90 |

| | | | |
|---|---|---|---|
| **Interval 18** | 96 | **Interval 41** | 96 |
| **Interval 19** | 95 | **Interval 42** | 89 |
| **Interval 20** | 96 | **Interval 43** | 95 |
| **Interval 21** | 95 | **Interval 44** | 88 |
| **Interval 22** | 96 | **Interval 45** | 90 |
| **Interval 23** | 96 | **Interval 46** | 90 |

In Fig. 4, box plots of all RV with a start and end reference of the astronomical seasons are shown. The typical evolution of the NDVI along a year can be seen together with the inter-quartile range.

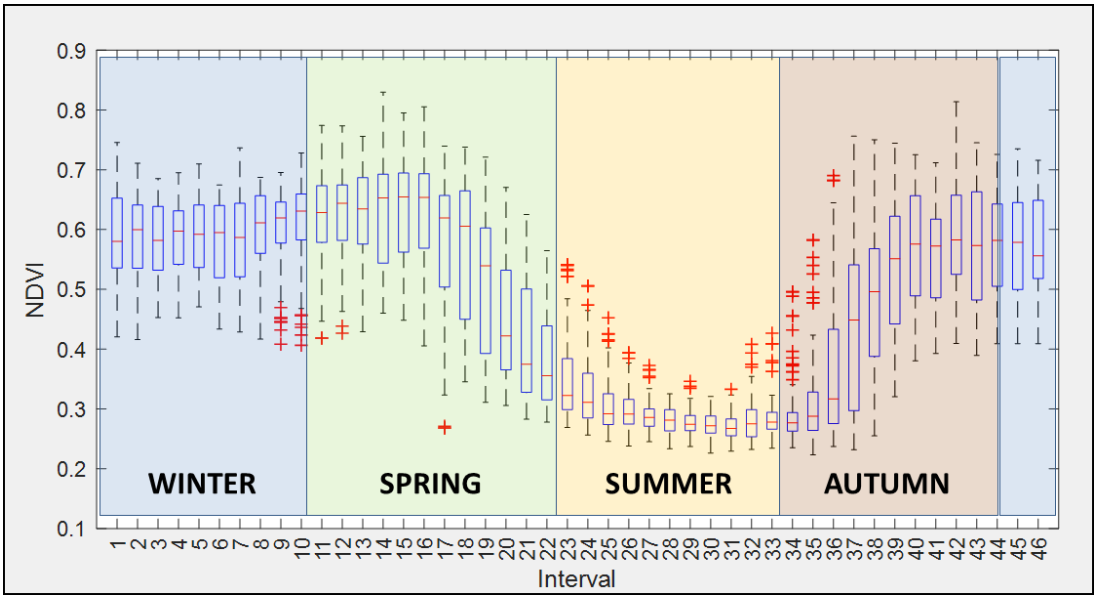


**Figure 4.** Box plots of 46 random variables (RV) are shown as well as start and end reference of every season. Study period from 2002 to 2017.

The observed evolution of NDVI through the different seasons is typical of the pasture in this area. The summer presents the lowest mean values which begin to increase in autumn achieving a maximum mean value of 0.60 or 0.65 during the beginning of spring. In the middle of the spring NDVI decrease again, approaching the lowest mean value of 0.28 approximately in summer.

Taking into account these values, dense vegetation, in this study pasture, is found from middle of October (interval 37) till the end of May (interval 19). It is in this period where the precipitation concentrates (see Table 1). During the summer, the NDVI mean values are lower than 0.3 corresponding with low precipitation and high temperatures.

Following the work of Escribano-Rodriguez et al. (2014), there is a relationship of pasture damage and a NDVI value around 0.40. Even if the authors point out that this value is highly variable depending on the location, we can see that summer season in this case study is under this value (see Fig. 4). This can explain that "Insurances for Damaged Pasture" usually do not apply in these dates due to the arid environment (BOE, 2013).

The statistical metric used in this study to assess the fit of the observed NDVI values with respect to the PDF candidates (Normal, Gamma, Beta and GEV) was the Chi square test ($\chi^2$ test). The following steps were carried out:

1. MLM was applied to model these 46 RV. Parameters were calculated for the four PDF candidates (see Table 2).
2. To check the goodness of the fit of PDF candidates, a Chi square test ($\chi^2$ test) was applied from 7 classes to 14 classes meeting the requirement that each class had at least five observations. The level of significance ($\alpha$) was fixed to 5% for all the candidates.

### *3.2.1* Maximum Likelihood Method

Table A1 at Appendix A shows the estimated parameters for each PDF and each interval calculated by the MLM. These parameters were used to compare the estimated PDF with the NDVI observed values on different times through the seasons. The following intervals are shown as examples of better GEV fit: interval 4 and 8 (for winter, see Fig. 5), interval 17 and 21 (for spring, see Fig. 6) and interval 36 and 40 (for autumn, see Fig. 7). In these plots, observed frequency is compared versus Normal and GEV density distributions calculated by MLM.

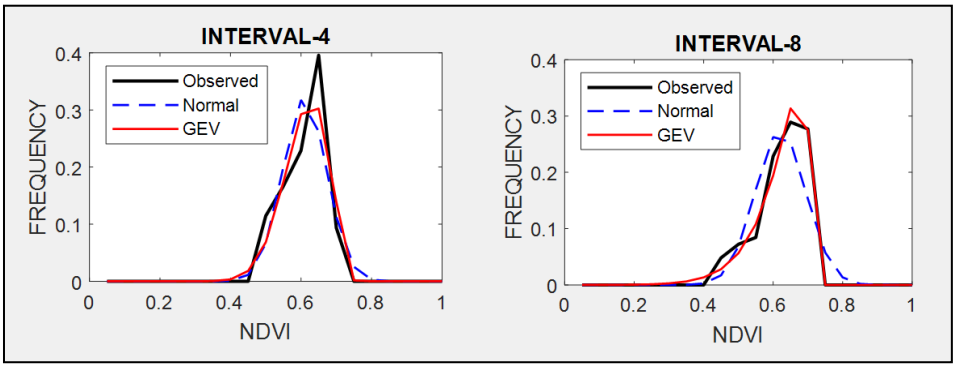


**Figure 5.** Comparison between observed NDVI frequency, GEV and Normal probability density functions (PDF) on two different dates. Intervals 4 and 8 are examples for winter.

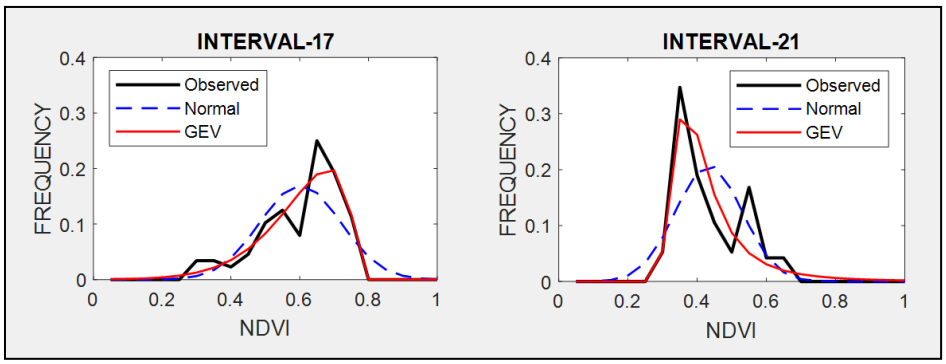


**Figure 6.** Comparison between observed NDVI frequency, GEV and Normal probability density functions (PDF) on two different dates. Intervals 17 and 21 are examples for spring.

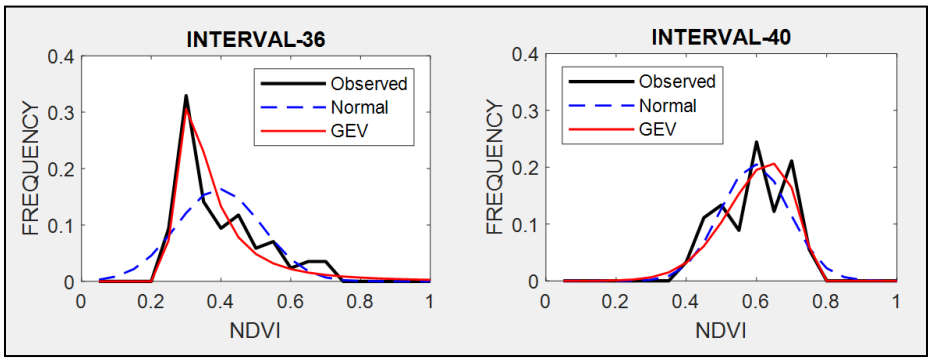


**Figure 7.** Comparison between observed NDVI frequency, GEV and Normal probability density functions (PDF) on two different times. Intervals 36 and 41 are examples for autumn.

During winter (see Fig. 5) the observed NDVI distribution presents negative skewness. Then, there is a higher frequency of high NDVI values corresponding with significant precipitation. During spring (see Fig. 6) an evolution in the skewness is observed passing from negative to positive, and so, the lower NDVI values become the higher probable. Finally, during autumn (see Fig. 7) precipitation begins and from positive pass to negative skewness and higher NDVI values are possible. We can observe that Normal distribution has no flexibility to follow this dynamic in the distributions on each time. This comparison is done in a sequential order for the whole of intervals in Figures A1, A2, A3 and A4 at Appendix A.

### *3.2.2* Chi square test

Twelve intervals (from 23 to 34) corresponding to the months of July, August and September have been excluded of this analysis since these intervals fall into the dry

season in the study area, normally not covered by any SIBI. Therefore, calculations were carried out over 34 intervals.

To assess the general goodness of fit, the number of intervals where the $\chi^2$ test was accepted (or failed to reject), were calculated for every PDF candidate. Then, the percentage of accepted intervals, over the total 34 intervals, was also calculated. Fig. 8 shows this percentage of intervals that fit for every PDF candidate. The number of classes used in $\chi^2$ test is represented at the X-axis (from 7 to 14 classes).

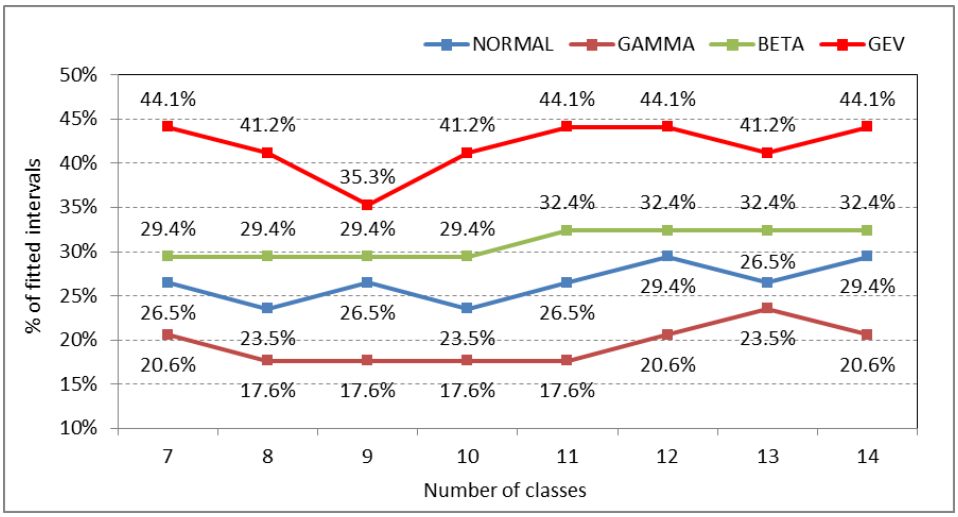


**Figure 8.** Percentage of fitted intervals (Y axis) for each PDF candidate (Normal, Gamma, Beta and GEV distributions) in function of the number of classes (X axis).

## 4. Discussion

### *4.1* Statistical context

Fig. 8 indicates that GEV distributions explain more intervals (more than 40% for the majority of the class analysis) than the Normal, Gamma or Beta distributions. An important difference between the Normal distribution and the PDFs used in this work is their skewness and kurtosis. Many of the observed NDVI distributions present a clear asymmetry and long tails in one or both sides that causes Normal distributions not to be the optimal fit.

There is a relationship between seasons and the number of intervals that fit correctly. We found that GEV distributions explain better intervals of spring and autumn since their

observed distributions are very asymmetric. On the other hand, we did not find an important difference in winter, since the observed distributions are mainly symmetric.

The more skewness and kurtosis depart from those of the Normal distribution the larger the errors affecting the insurance designed based on Normal distributions (Turvey et al., 2012). It is an expected result as pasture cultivation is quite different from the development of arable crops, where Normal distributions in the NDVI values are more common. This high heterogeneity in time and space of NDVI estimated on pasture has been pointed out in several works (Martin-Sotoca et al, 2018). At the same time, the more different the observed NDVI frequency is from a Normal distribution, the less representative is the average, and so, the median becomes a more representative value.

### *4.2* Insurance context

The use of NDVI thresholds in damaged pasture context was presented in the introduction section, being an example of using the "Insurance for Damaged Pasture" in Spain (BOE, 2013). We have chosen this last insurance to compare the results between applying Normal and GEV distribution methodologies. In this particular case the NDVI threshold ($NDVI_{th}$) was calculated using the expression $NDVI_{th} = \mu - k \cdot \sigma$ (where $\mu, \sigma$ are average and standard deviation of NDVI distributions respectively, assuming the Normal hypothesis).

The probability of being below $NDVI_{th}$ (using $k = 0.7$, first damage level in the insurance) at every interval has been calculated assuming the Normal hypothesis. As it was expected, this value is always 24.2% (see third column in Table 4). The probability of being below $NDVI_{th}$ has also been calculated using GEV distributions obtained in this study. The probability obtained by GEV distributions is mostly lower than the Normal distributions in spring, autumn and winter (see Table 4) that is the working period of the insurance.

Observing where in time are the highest relative errors in probabilities (fifth column in Table 4), intervals corresponding to the end of winter, second middle of spring and the beginning of autumn present errors higher than 10%. This could explain why it is in spring and autumn when more disagreements exist between farmers and insurance company in claims.

**Table 4 – First column:** time intervals of approximately 8 days along the year. **Second column:** NDVI thresholds ($NDVI_{th}$) based on a Normal distribution applying $\mu - 0.7 \times \sigma$. **Third column:** percentages of

556 area below the $NDVI_{th}$ when Normal distributions are applied. **Fourth column:** percentages of area
557 below the $NDVI_{th}$ when GEV distributions are applied. **Fifth column:** relative area error of GEV
558 compared to the Normal distribution.

559

| RANDOM VARIABLE | NORMAL | | GEV | |
|---|---|---|---|---|
| | $NDVI_{th}$ | Prob. | Prob. | Error (%) |
| **Interval 1** | 0.535 | 24.20% | 24.37% | 0.70% |
| **Interval 2** | 0.541 | 24.20% | 23.18% | -4.21% |
| **Interval 3** | 0.541 | 24.20% | 23.27% | -3.84% |
| **Interval 4** | 0.543 | 24.20% | 23.27% | -3.84% |
| **Interval 5** | 0.545 | 24.20% | 24.17% | -0.12% |
| **Interval 6** | 0.534 | 24.20% | 21.48% | -11.24% |
| **Interval 7** | 0.528 | 24.20% | 24.01% | -0.79% |
| **Interval 8** | 0.546 | 24.20% | 20.70% | -14.46% |
| **Interval 9** | 0.555 | 24.20% | 21.30% | -11.98% |
| **Interval 10** | 0.561 | 24.20% | 22.28% | -7.93% |
| **Interval 11** | 0.567 | 24.20% | 23.49% | -2.93% |
| **Interval 12** | 0.572 | 24.20% | 23.75% | -1.86% |
| **Interval 13** | 0.571 | 24.20% | 23.20% | -4.13% |
| **Interval 14** | 0.570 | 24.20% | 24.29% | 0.37% |
| **Interval 15** | 0.571 | 24.20% | 23.47% | -3.02% |
| **Interval 16** | 0.560 | 24.20% | 23.26% | -3.88% |
| **Interval 17** | 0.495 | 24.20% | 21.29% | -12.02% |
| **Interval 18** | 0.484 | 24.20% | 21.58% | -10.83% |
| **Interval 19** | 0.442 | 24.20% | 23.06% | -4.71% |
| **Interval 20** | 0.381 | 24.20% | 27.20% | 12.40% |
| **Interval 21** | 0.342 | 24.20% | 29.46% | 21.74% |
| **Interval 22** | 0.323 | 24.20% | 28.84% | 19.17% |
| **Interval 35** | 0.257 | 24.20% | 18.98% | -21.57% |
| **Interval 36** | 0.285 | 24.20% | 28.57% | 18.06% |
| **Interval 37** | 0.333 | 24.20% | 25.90% | 7.02% |
| **Interval 38** | 0.398 | 24.20% | 24.27% | 0.29% |
| **Interval 39** | 0.454 | 24.20% | 23.79% | -1.69% |
| **Interval 40** | 0.503 | 24.20% | 22.81% | -5.74% |
| **Interval 41** | 0.491 | 24.20% | 23.23% | -4.01% |
| **Interval 42** | 0.517 | 24.20% | 24.66% | 1.90% |
| **Interval 43** | 0.507 | 24.20% | 23.13% | -4.42% |

| | | | | |
|---|---|---|---|---|
| **Interval 44** | 0.514 | 24.20% | 23.49% | -2.93% |
| **Interval 45** | 0.515 | 24.20% | 23.70% | -2.07% |
| **Interval 46** | 0.509 | 24.20% | 23.33% | -3.60% |

560

561 An alternative calculation can be the use of Normal probability (24.2%) to calculate new
562 $\boldsymbol{NDVI_{th}}$ based on GEV (see Table 5). It can be seen that new $\boldsymbol{NDVI_{th}}$ obtained by GEV
563 distributions are mostly higher than thresholds using Normal distributions in spring,
564 autumn and winter. Considering these results we find that damage thresholds calculated
565 by GEV distributions are mostly above the ones calculated by Normal distributions.

566 Again, intervals corresponding to the end of winter, second middle of spring and the
567 beginning of autumn present $\boldsymbol{NDVI_{th}}$ relative errors higher than 1% in absolute values
568 (fourth column in Table 5).

569

570 **Table 5 - First column:** time intervals of approximately 8 days along the year. **Second column:** NDVI
571 thresholds ($NDVI_{Th}$) based on a Normal distribution (Normal) applying $\mu - 0.7 \times \sigma$. **Third column:**
572 $NDVI_{Th}$ based on a GEV distribution (GEV) using 24.2% as the area below the $NDVI_{Th}$. **Fourth column:**
573 relative $NDVI_{Th}$ error of GEV compared to the Normal distribution.

574

| RANDOM VARIABLE | $NDVI_{Th}$ | | |
|---|---|---|---|
| | Normal | GEV | Error (%) |
| **Interval 1** | 0.535 | 0.534 | -0,19% |
| **Interval 2** | 0.541 | 0.543 | 0,37% |
| **Interval 3** | 0.541 | 0.543 | 0,37% |
| **Interval 4** | 0.543 | 0.545 | 0,37% |
| **Interval 5** | 0.545 | 0.545 | 0,00% |
| **Interval 6** | 0.534 | 0.543 | 1,69% |
| **Interval 7** | 0.528 | 0.528 | 0,00% |
| **Interval 8** | 0.546 | 0.558 | 2,20% |
| **Interval 9** | 0.555 | 0.563 | 1,44% |
| **Interval 10** | 0.561 | 0.567 | 1,07% |
| **Interval 11** | 0.567 | 0.569 | 0,35% |
| **Interval 12** | 0.572 | 0.574 | 0,35% |
| **Interval 13** | 0.571 | 0.574 | 0,53% |
| **Interval 14** | 0.570 | 0.569 | -0,18% |
| **Interval 15** | 0.571 | 0.573 | 0,35% |
| **Interval 16** | 0.560 | 0.563 | 0,54% |

| | | | |
|---|---|---|---|
| **Interval 17** | 0.495 | 0.510 | 3,03% |
| **Interval 18** | 0.484 | 0.498 | 2,89% |
| **Interval 19** | 0.442 | 0.447 | 1,13% |
| **Interval 20** | 0.381 | 0.374 | -1,84% |
| **Interval 21** | 0.342 | 0.334 | -2,34% |
| **Interval 22** | 0.323 | 0.318 | -1,55% |
| **Interval 35** | 0.257 | 0.262 | 1,95% |
| **Interval 36** | 0.285 | 0.278 | -2,46% |
| **Interval 37** | 0.333 | 0.327 | -1,80% |
| **Interval 38** | 0.398 | 0.398 | 0,00% |
| **Interval 39** | 0.454 | 0.455 | 0,22% |
| **Interval 40** | 0.503 | 0.508 | 0,99% |
| **Interval 41** | 0.491 | 0.494 | 0,61% |
| **Interval 42** | 0.517 | 0.516 | -0,19% |
| **Interval 43** | 0.507 | 0.510 | 0,59% |
| **Interval 44** | 0.514 | 0.516 | 0,39% |
| **Interval 45** | 0.515 | 0.516 | 0,19% |
| **Interval 46** | 0.509 | 0.511 | 0,39% |

## 5. Conclusions

According to the results obtained in the study area using MLM and $\chi^2$ test, it can be concluded that Normal distributions are not a good fit to the NDVI observations, and GEV distributions provide a better approximation.

The difference between Normal and GEV assumption is more evident in the transition from winter to summer (spring), where NDVI values decrease, and then from summer to winter (autumn) presenting the opposite behavior of increasing NDVI values. In both periods asymmetrical distributions were found, negative skewness for the spring transition and positive skewness for the autumn transition. During both periods the variability in precipitation and temperatures were higher in this location.

We have found differences if GEV assumption is selected instead of the Normal one when defining damaged pasture thresholds ($NDVI_{th}$). The use of these different assumptions should be taken into account in future insurance implementations due to the important consequences of supposing a damage event or not. We propose the use of

quantiles in observed NDVI distributions instead of average and standard deviation, typically of Normal distributions, to calculate new $NDVI_{th}$.

## Acknowledgements

This research has been partially supported by funding from MINECO under contract No. MTM2015-63914-P and CICYT PCIN-2014-080.

# Appendix A

**Table A1 -** Maximum Likelihood parameters calculated for 4 PDF.

| RANDOM VARIABLE | NORMAL | | GAMMA | | BETA | | GEV | | |
|---|---|---|---|---|---|---|---|---|---|
| | $\mu$ | $\sigma$ | $\alpha$ | $\beta$ | a | b | $\mu$ | $\sigma$ | $\xi$ |
| **Interval 1** | 0.591 | 0.081 | 53.31 | 0.011 | 21.45 | 14.82 | 0.563 | 0.080 | -0.297 |
| **Interval 2** | 0.589 | 0.069 | 71.14 | 0.008 | 30.62 | 21.40 | 0.571 | 0.073 | -0.477 |
| **Interval 3** | 0.583 | 0.060 | 94.15 | 0.006 | 39.56 | 28.34 | 0.567 | 0.063 | -0.457 |
| **Interval 4** | 0.585 | 0.060 | 91.88 | 0.006 | 39.58 | 28.05 | 0.570 | 0.064 | -0.468 |
| **Interval 5** | 0.588 | 0.061 | 93.92 | 0.006 | 38.83 | 27.25 | 0.568 | 0.061 | -0.340 |
| **Interval 6** | 0.582 | 0.068 | 70.28 | 0.008 | 30.67 | 22.05 | 0.577 | 0.083 | -0.846 |
| **Interval 7** | 0.584 | 0.080 | 52.52 | 0.011 | 22.16 | 15.82 | 0.559 | 0.082 | -0.366 |
| **Interval 8** | 0.596 | 0.071 | 65.37 | 0.009 | 28.89 | 19.59 | 0.591 | 0.081 | -0.833 |
| **Interval 9** | 0.601 | 0.066 | 76.02 | 0.008 | 34.31 | 22.84 | 0.590 | 0.070 | -0.652 |
| **Interval 10** | 0.613 | 0.073 | 63.83 | 0.010 | 27.80 | 17.62 | 0.598 | 0.079 | -0.572 |
| **Interval 11** | 0.621 | 0.078 | 58.72 | 0.011 | 24.33 | 14.86 | 0.600 | 0.083 | -0.451 |
| **Interval 12** | 0.624 | 0.073 | 68.33 | 0.009 | 28.01 | 16.94 | 0.603 | 0.078 | -0.431 |
| **Interval 13** | 0.624 | 0.075 | 66.22 | 0.009 | 26.23 | 15.85 | 0.604 | 0.080 | -0.476 |
| **Interval 14** | 0.631 | 0.088 | 50.23 | 0.013 | 18.71 | 10.92 | 0.603 | 0.090 | -0.342 |
| **Interval 15** | 0.630 | 0.084 | 53.60 | 0.012 | 21.17 | 12.45 | 0.607 | 0.089 | -0.448 |
| **Interval 16** | 0.627 | 0.096 | 38.75 | 0.016 | 16.08 | 9.59 | 0.602 | 0.103 | -0.474 |
| **Interval 17** | 0.577 | 0.117 | 20.47 | 0.028 | 10.24 | 7.58 | 0.560 | 0.127 | -0.692 |
| **Interval 18** | 0.568 | 0.120 | 20.52 | 0.028 | 9.71 | 7.42 | 0.552 | 0.136 | -0.718 |
| **Interval 19** | 0.523 | 0.116 | 19.46 | 0.027 | 9.52 | 8.68 | 0.495 | 0.125 | -0.493 |
| **Interval 20** | 0.452 | 0.101 | 20.99 | 0.022 | 10.98 | 13.31 | 0.401 | 0.077 | 0.078 |
| **Interval 21** | 0.409 | 0.095 | 19.94 | 0.021 | 11.18 | 16.13 | 0.354 | 0.060 | 0.325 |
| **Interval 22** | 0.379 | 0.080 | 24.66 | 0.015 | 14.41 | 23.52 | 0.333 | 0.046 | 0.385 |
| **Interval 23** | 0.353 | 0.073 | 26.54 | 0.013 | 15.85 | 29.01 | 0.311 | 0.036 | 0.456 |
| **Interval 24** | 0.328 | 0.056 | 38.36 | 0.009 | 24.22 | 49.65 | 0.298 | 0.033 | 0.287 |
| **Interval 25** | 0.305 | 0.044 | 53.52 | 0.006 | 35.62 | 81.20 | 0.282 | 0.028 | 0.210 |
| **Interval 26** | 0.298 | 0.034 | 78.93 | 0.004 | 54.47 | 128.55 | 0.283 | 0.029 | -0.064 |
| **Interval 27** | 0.289 | 0.026 | 126.85 | 0.002 | 88.33 | 217.15 | 0.278 | 0.021 | -0.030 |
| **Interval 28** | 0.282 | 0.022 | 166.17 | 0.002 | 119.50 | 305.03 | 0.274 | 0.022 | -0.322 |
| **Interval 29** | 0.278 | 0.021 | 179.09 | 0.002 | 127.93 | 332.63 | 0.269 | 0.018 | -0.085 |
| **Interval 30** | 0.273 | 0.019 | 203.11 | 0.001 | 147.67 | 393.21 | 0.266 | 0.019 | -0.247 |
| **Interval 31** | 0.272 | 0.022 | 166.83 | 0.002 | 120.11 | 321.95 | 0.262 | 0.018 | -0.059 |
| **Interval 32** | 0.280 | 0.034 | 75.63 | 0.004 | 52.36 | 134.30 | 0.264 | 0.023 | 0.118 |
| **Interval 33** | 0.285 | 0.034 | 82.05 | 0.004 | 54.90 | 137.68 | 0.270 | 0.020 | 0.122 |
| **Interval 34** | 0.295 | 0.057 | 33.26 | 0.009 | 21.15 | 50.37 | 0.268 | 0.024 | 0.363 |

| | | | | | | | | | |
|---|---|---|---|---|---|---|---|---|---|
| **Interval 35** | 0.312 | 0.079 | 19.70 | 0.016 | 11.83 | 25.94 | 0.275 | 0.038 | 0.300 |
| **Interval 36** | 0.369 | 0.121 | 10.81 | 0.034 | 6.11 | 10.33 | 0.298 | 0.063 | 0.480 |
| **Interval 37** | 0.432 | 0.141 | 9.45 | 0.046 | 5.21 | 6.81 | 0.370 | 0.120 | -0.080 |
| **Interval 38** | 0.487 | 0.128 | 13.88 | 0.035 | 7.25 | 7.63 | 0.445 | 0.127 | -0.321 |
| **Interval 39** | 0.529 | 0.107 | 23.56 | 0.022 | 11.39 | 10.16 | 0.497 | 0.110 | -0.390 |
| **Interval 40** | 0.570 | 0.096 | 34.02 | 0.017 | 15.10 | 11.40 | 0.548 | 0.105 | -0.533 |
| **Interval 41** | 0.554 | 0.090 | 36.42 | 0.015 | 16.90 | 13.64 | 0.531 | 0.096 | -0.471 |
| **Interval 42** | 0.583 | 0.095 | 37.29 | 0.016 | 15.56 | 11.11 | 0.551 | 0.094 | -0.295 |
| **Interval 43** | 0.574 | 0.097 | 34.27 | 0.017 | 14.93 | 11.07 | 0.550 | 0.103 | -0.482 |
| **Interval 44** | 0.572 | 0.083 | 47.13 | 0.012 | 20.40 | 15.26 | 0.549 | 0.086 | -0.425 |
| **Interval 45** | 0.576 | 0.088 | 42.59 | 0.014 | 18.17 | 13.36 | 0.550 | 0.090 | -0.396 |
| **Interval 46** | 0.570 | 0.088 | 41.98 | 0.014 | 18.11 | 13.66 | 0.546 | 0.092 | -0.445 |

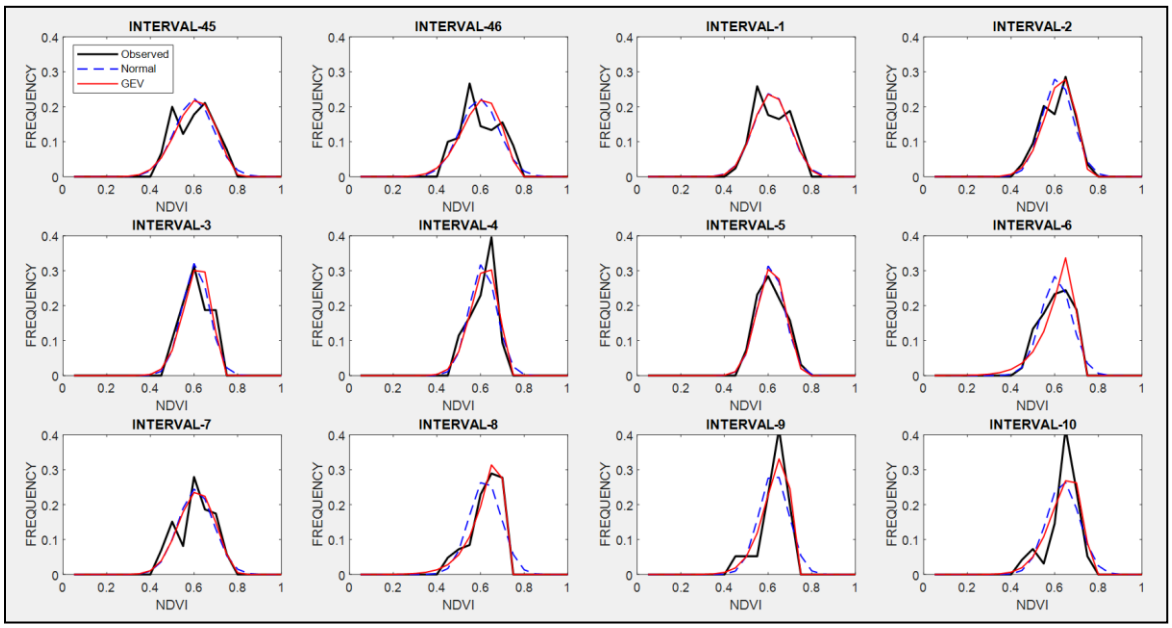


**Figure A1.** Observed NDVI, GEV and Normal probability density functions (PDF) from interval 45 to interval 10 (from 19 December to 21 March) representing winter.

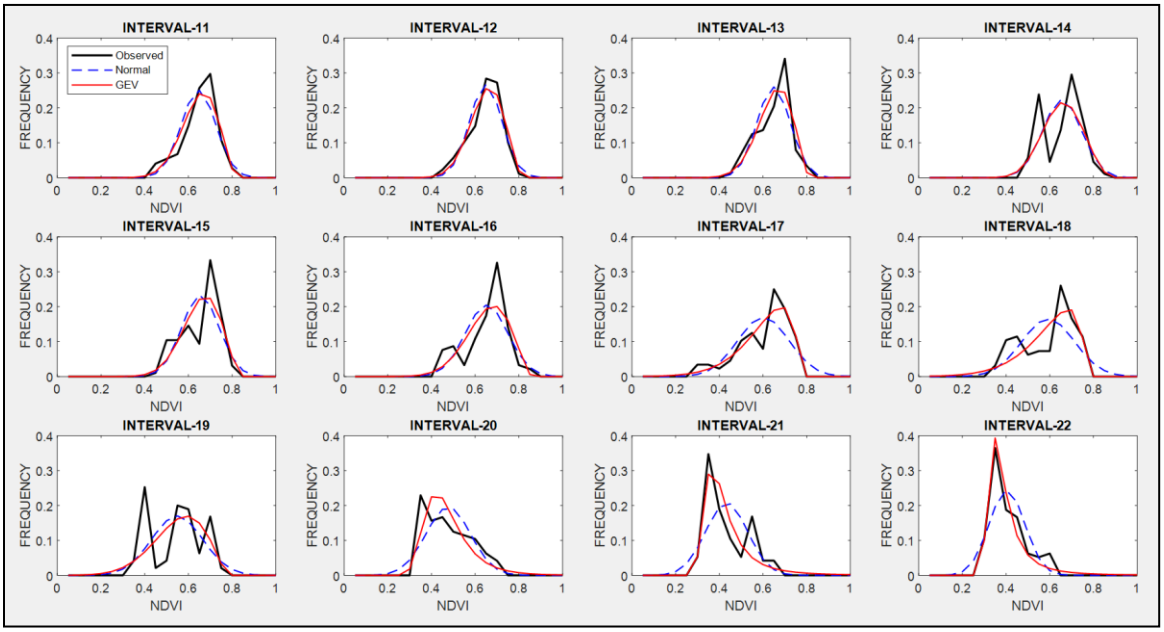


611

612 **Figure A2.** Observed NDVI, GEV and Normal probability density functions (PDF) from interval 11 to
613 interval 22 (from 22 March to 25 June) representing spring.

614

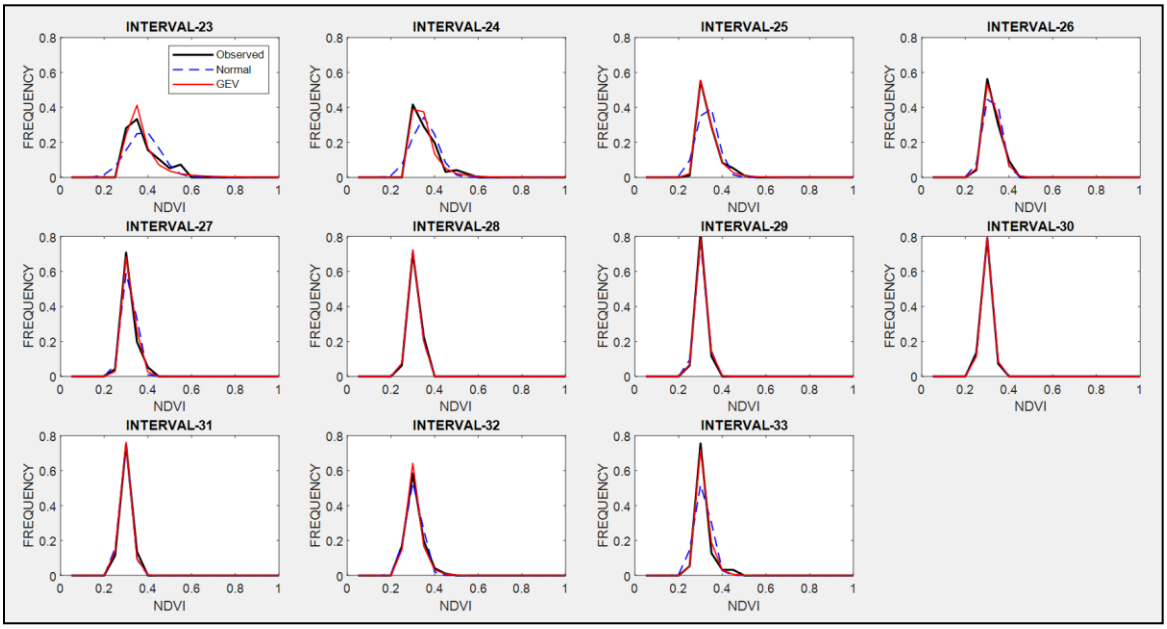


615

616 **Figure A3.** Observed NDVI, GEV and Normal probability density functions (PDFs) from interval 23
617 to interval 33 (from 26 June to 21 September) representing summer.

618

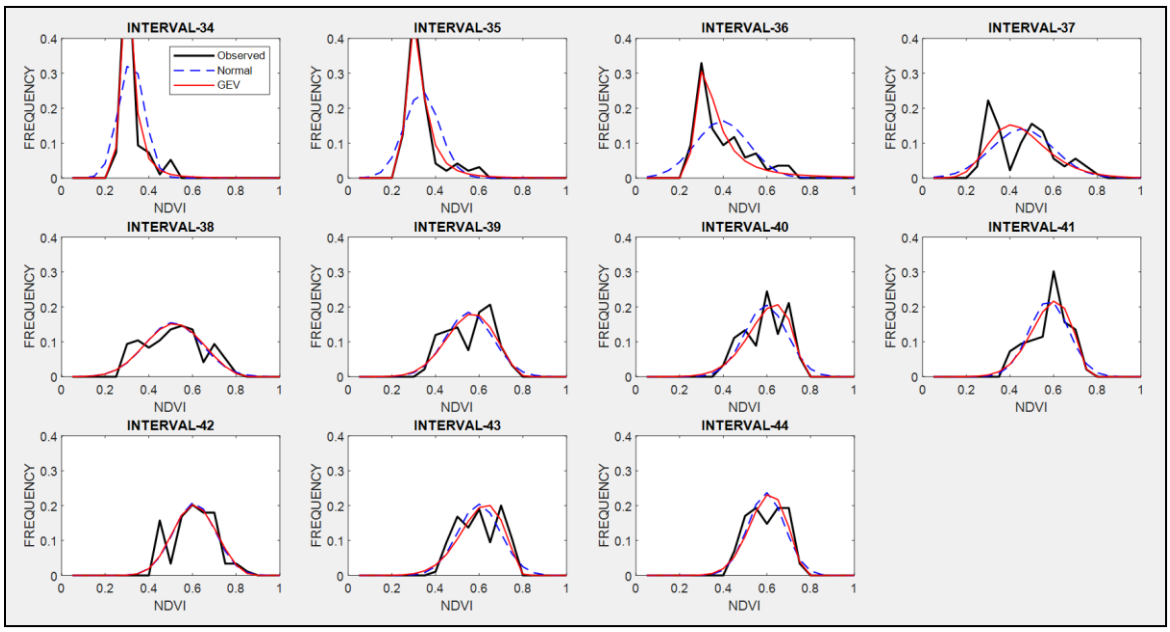


619

620 **Figure A4.** Observed NDVI, GEV and Normal PDFs from interval 34 to interval 44 (from 22
621 September to 18 December) representing autumn.

622

## References


Agencia Estatal de Meteorología (AEMET). Available at: www.aemet.es, 2017.

Al-Bakri, J. T., and Taylor, J. C.: Application of NOAA AVHRR for monitoring vegetation conditions and biomass in Jordan, J. Arid Environ, 54, 579–593, 2003.

Anyamba, A., and Tucker, C.J.: Historical perspective of AVHRR NDVI and vegetation drought monitoring. In: Remote Sensing of Drought: Innovative Monit Approaches, pp. 23, 2012.

Bailey, S.: The Impact of Cash Transfers on Food Consumption in Humanitarian Settings: A review of evidence, Study for the Canadian Foodgrains Bank, May 2013.

Bayarjargal, Y., Karnieli, A., Bayasgalan, M., Khudulmur, S., Gandush, C., and Tucker, C.J.: A comparative study of NOAA-AVHRR derived drought indices using change vector analysis, Remote Sens. Environ. 105 (1), 9–22, 2006.

Boletin Oficial del Estado (BOE, 6638 - Orden AAA/1129/2013. Nº 145, III, p-46077, 2013.

Cochran, William G.: The Chi-square Test of Goodness of Fit, Annals of Mathematical Statistics. 23: 315–345, 1952.

Crimmins, M. A., and Crimmins T. M.: Monitoring plant phenology using digital repeat photography, Environ. Manage, 41, 949-958, 2008.

Dalezios, N. R., Blanta, A., Spyropoulos, N. V., and Tarquis A. M.: Risk identification of agricultural drought for sustainable Agroecosystems, Nat. Hazards Earth Syst. Sci., 14, 2435–2448, 2014.

Dalezios, N. R.: The Role of Remotely Sensed Vegetation Indices in Contemporary Agrometeorology. Invited paper in Honorary Special Volume in memory of late Prof. A. Flokas. Publisher: Hellenic Meteorological Association, 33-44, 2013.

De Leeuw, J., Vrieling, A., Shee, A., Atzberger, C., Hadgu, K. M., Biradar, C. M., Humphrey Keah, H., and Turvey, C.: The Potential and Uptake of Remote Sensing in Insurance: A Review, Remote Sens., 6(11), 10888-10912, 2014.

Escribano Rodríguez, J. Agustín, Díaz-Ambrona, Carlos Gregorio H., and Tarquis Alfonso, Ana María: Selection of vegetation indices to estimate pasture production in Dehesas, PASTOS, 44(2), 6-18, 2014.

Fensholt, R., and Proud, S. R.: Evaluation of earth observation based global long term vegetation trends - comparing GIMMS and MODIS global NDVI time series, Remote Sens. Environ., 119, 131–147, 2012.

Flynn E. S.: Using NDVI as a pasture management tool. Master Thesis, University of Kentucky, 2006.

Forkel, M., Carvalhais, N., Verbesselt, J., Mahecha, M.D., Neigh, C. S., and Reichstein, M.: Trend change detection in NDVI time series: effects of inter-annual variability and methodology, Remote Sens., 5, pp, 2113–2144, 2013.

661 Fuller, D.O.: Trends in NDVI time series and their relation to rangeland and crop production
662 in Senegal, 1987–1993, Int. J. Remote Sens., 19, 2013–2018, 1998.
663 Gommes, R., and Kayitakire, F.: The challenges of index-based insurance for food security
664 in developing countries. Proceedings, Technical Workshop, JRC, Ispra, 2-3 May 2012.
665 Publisher: JRC-EC, p. 276, 2013.
666 Gouveia, C., Trigo, R. M., and Da Camara, C. C.: Drought and vegetation stress monitoring
667 in Portugal using satellite data, Nat. Hazards Earth Syst. Sci., 9, 185-195, 2009.
668 Goward, S. N., Tucker, C. J., and Dye, D.G.: North-American vegetation patterns observed
669 with the NOAA-7 advanced very high-resolution radiometer. Vegetation, 64, 3–14,
670 1985.
671 Graham, E. A., Yuen, E. M., Robertson, G. F., Kaiser, W. J., Hamilton, M. P., and Rundel, P.
672 W.: Budburst and leaf area expansion measured with a novel mobile camera system
673 and simple color thresholding, Environ. Exp. Bot., 65, 238-244, 2009.
674 Hobbs, T. J.: The use of NOAA-AVHRR NDVI data to assess herbage production in the arid
675 rangelands of central Australia, Int. J. Remote Sens., 16, 1289–1302, 1995.
676 Holben, B. N.: Characteristics of maximum-value composite images from temporal AVHRR
677 data, Int. J. Remote Sens., 7, 1417–1434, 1986.
678 Kottek, M., Grieser, J., Beck, C., Rudolf, B., and Rubel, F.: World Map of the Köppen-Geiger
679 climate classification updated, Meteorologische Zeitschrift, 15, 259-263, 2006.
680 Kundu, A., Dwivedi, S., and Dutta, D.: Monitoring the vegetation health over India during
681 contrasting monsoon years using satellite remote sensing indices, Arab J Geosci., 9,
682 144, 2016.
683 Land Processes Distributed Active Archive Center (LP DAAC): Surface Reflectance 8-Day L3
684 Global 500m. NASA and USGS. Available at:
685 https://lpdaac.usgs.gov/products/modis_products_Table/mod09a1. 2014.
686 Larson, H. J.: Introduction to Probability Theory and Statistical Inference (3rd edition). New
687 York, John Wiley and Sons, 1982.
688 Leblois, A.: Weather index-based insurance in a cash crop regulated sector: ex ante
689 evaluation for cotton producers in Cameroon. Paper presented at the JRC/IRI
690 workshop on The Challenges of Index-Based Insurance for Food Security in Developing
691 Countries, Ispra, 2-3, May, 2012.
692 Lovejoy, S., Tarquis, A. M., Gaonac'h, H., and Schertzer, D.: Single and Multiscale remote
693 sensing techniques, multifractals and MODIS derived vegetation and soil moisture.
694 Vadose Zone J., 7, 533-546, 2008.
695 Li, R., Tsunekawa, A., and Tsubo, M.: Index-based assessment of agricultural drought in a
696 semi-arid region of Inner Mongolia, China, J. Arid Land 6 (1), 3–15, 2014.

Maples, J. G., Brorsen, B. W., and Biermaches, J. T.: The rainfall Index Annual Forage pilot program as a risk management tool for cool-season forage. J. Agr. Appl Econ, 48(1), 29–51, 2016.

Martin-Sotoca, J. J., Saa-Requejo, A., Orondo J. B., and Tarquis, A. M.: Singularity maps applied to a vegetation index, Bio. Eng. 168, 42-53, 2018.

Motohka, T., Nasahara, K. N., Murakami, K., and Nagai, S.: Evaluation of sub-pixel cloud noises on MODIS daily spectral indices based on in situ measurements, Remote Sens., 3, 1644–1662, 2011.

Nanzad, L., Zhang, J., Tuvdendorj, B., Nabil, M., Zhang, S., and Bai, Y.: NDVI anomaly for drought monitoring and its correlation with climate factors over Mongolia from 2000 to 2016, Journal of Arid Environments Volume 164, Pages 69-77, 2019.

Niemeyer, S.: New drought indices, First Int. Conf. on Drought Management: Scientific and Technological Innovations, Zaragoza, Spain. Joint Research Centre of the European Commission, Available online at http://www.iamz.ciheam.org/medroplan/zaragoza2008/Sequia2008/Session3/S.Niemeyer.pdf, 2008.

Ortega-Farias, S., Ortega-Salazar, S., Poblete, T., Kilic, A., Allen,R., Poblete-Echeverría, C., Ahumada-Orellana, L., Zuñiga,M., and Sepúlveda, D.: Estimation of Energy Balance Components over a Drip-Irrigated Olive Orchard Using Thermal and Multispectral Cameras Placed on a Helicopter-Based Unmanned Aerial Vehicle (UAV), Remote Sens., 8, 638, pp 18, 2016.

Park, S.: Cloud and cloud shadow effects on the MODIS vegetation index composites of the Korean Peninsula, Int. J. Remote Sens., 34, 1234–1247, 2013.

Peters, A. J., E. A. Walter-Shea, L. Ji, A. Vina, M. Hayes, and M.D. Svoboda: Drought monitoring with NDVI-Based Standardized Vegetation Index, Photogrammetric Engineering and Remote Sensing S 68:71–75, 2002.

Rao, K. N.: Index based Crop Insurance, Agric. Agric. Sci. Proc., 1, 193–203, 2010.

Roumiguié, A., Sigel, G., Poilvé, H., Bouchard, B., Vrieling, A., and Jacquin, A.: Insuring forage through satellites: testing alternative indices against grassland production estimates for France, Int. J. Remote Sens., 38, 1912-1939, 2017.

Roumiguié, A., Jacquin, A., Sigel, G., Poilvé, H., Lepoivre, B., and Hagolle, O.: Development of an index-based insurance product: validation of a forage production index derived from medium spatial resolution fCover time series, GIScience Remote Sens., 52, 94-113, 2015.

Tackenberg, Oliver: A New Method for Non-destructive Measurement of Biomass, Growth Rates, Vertical Biomass Distribution and Dry Matter Content Based on Digital Image Analysis, Annals of Botany, 99(4), 777–783, 2007.

Turvey, C. G., and Mcaurin, M. K.: Applicability of the Normalized Difference Vegetation Index (NDVI) in Index-Based Crop Insurance Design, Am. Meorol. Soc., 4, 271-284, 2012.

UNEP Word Atlas of Desertification: Second Ed. United Nations Enviroment Programe, Nairobi, 1997.

USDA. U.S. Department of Agriculture, Federal Crop Insurance Corporation, Risk Management Agency: Rainfall Index Plan Annual Forage Crop Provisions. 16- RI-AF. http://www.rma.usda.gov/policies/ri-vi/2015/16riaf.pdf 2013 (Accessed March 1, 2018).

Wei, W., Wu, W., Li, Z., Yang, P., and Qingbo Zhou, Q.: Selecting the Optimal NDVI Time-Series Reconstruction Technique for Crop Phenology Detection, Intell. Autom. Soft. Co. 22, 237-247, 2016.